HHS Public Access

Author manuscript

Hepatology. Author manuscript; available in PMC 2022 July 01.

Published in final edited form as:

Hepatology. 2021 July ; 74(1): 41–54. doi:10.1002/hep.31656.

Inhibition of long noncoding RNA Linc-Pint by hepatitis C virus in infected hepatocytes enhances lipogenesis

Mousumi Khatun[1], **Subhayan Sur**[1], **Robert Steele**[1], **Ranjit Ray**[2], **Ratna B. Ray**[1]

[1]Department of Pathology, Saint Louis University, Missouri, USA

[2]Department of Internal Medicine, Saint Louis University, Missouri, USA

Abstract

Background and Aims—Hepatitis C virus (HCV) often causes chronic infection in liver, cirrhosis, and in some instances, hepatocellular carcinoma (HCC). HCV encodes several factors those impair host genes for establishment of chronic infection. The long non-coding RNAs (lncRNAs) display diverse effects on biological regulations. However, their role in virus replication and underlying diseases are poorly understood. In this study, we have shown that HCV exploits lncRNA Linc-Pint in hepatocytes for enhancement of lipogenesis.

Approach and Results—We identified a lncRNA, Linc-Pint, which is significantly downregulated in HCV replicating hepatocytes and infected patient liver specimens. Using RNA-pull down-proteomics, we identified serine/arginine protein specific kinase 2 (SRPK2) as an interacting partner of Linc-Pint. Subsequent study demonstrated that overexpression of Linc-Pint inhibits the expression of lipogenesis related genes, such as FASN and ACLY. We also observed that Linc-Pint significantly inhibits HCV replication. Further, HCV mediated enhanced lipogenesis can be controlled by exogenous Linc-Pint expression. Together our results suggested that HCV mediated downregulation of Linc-Pint enhances lipogenesis favouring virus replication and liver disease progression.

Conclusions—We have shown that SRPK2 is a direct target of Linc-Pint and depletion of SRPK2 inhibits lipogenesis. Our study contributes to the mechanistic understanding of the previously unexplored role of Linc-Pint in HCV associated liver pathogenesis.

Keywords

Hepatitis C virus; Linc-Pint; SRPK2; FASN; Lipogenesis

Hepatitis C virus (HCV) infection is an important factor in the etiology of fibrosis/cirrhosis and hepatocellular carcinoma (HCC), and 1.3 million new cases of HCV is estimated in 2020 (1). HCV is a positive-strand RNA virus and does not integrate into the host genome.

Address correspondence to Ratna B. Ray, Department of Pathology, Saint Louis University, DRC 207, 1100 South Grand Boulevard, St. Louis, MO 63104. Phone: 314-977-7822; Fax: 314-771-3816; ratna.ray@health.slu.edu.

Author Contributions

M.K., S.S., R.R. and R.B.R. conceived the project. M.K., S.S. and R.S. helped acquisition and analysis of data. M.K., S.S. R.R. and R.B.R wrote the manuscript, and all authors edited the manuscript. R.B.R supervised the project, and R.R. and R.B.R provided funding for this study.

Potential conflict of interest: Nothing to report.

Host immune system fails to clear the infection in ~80% of the HCV infected individuals (2). Current anti-HCV drugs reduce viremia at the undetectable level, however, they do not prevent reinfection. Since HCV infection is often asymptomatic, infected individuals are diagnosed much later and in most of the cases they develop chronic infection. The HCV encodes different structural and non-structural proteins and regulates different non-coding RNAs that favour viral replication, host cell proliferation, survival, inflammation, and metabolism (2–4). Thus, in-depth understanding of the HCV pathogenesis at the molecular level has high importance.

Transcriptome studies and genome tiling arrays suggested a large number of genome (more than 90%) transcribes non-coding RNAs (1–3). Long non-coding RNAs (lncRNAs) are >200 nucleotides in length with no significant protein-coding potential. LncRNAs bind to DNA, RNA, or proteins and exert their functions in regulating different biological processes, like transcription, mRNA stabilization, and protein translation. Aberrant lncRNA expression has been observed in various cancers (4–6). The expression of lncRNAs were significantly different in cirrhosis and HCC as compared to preneoplastic tissues or adjacent non-tumor tissues (7).

Deregulation of cellular lncRNAs were seen in many types of viral infection like HBV, HIV and influenza in response to viral replication and pathogenesis (8). Similarly, transcriptome analysis of HCV infected hepatocytes revealed alteration in number of lncRNAs (8, 9). HCV-activated PKR induces lncRNA EGOT, which in turn decreases ISG expression, and favors HCV replication (9). LncRNA-GAS5 is induced by HCV, interestingly, this lncRNA inhibits HCV infection by binding with HCV NS3 protein (10), while IFN inducible lncRNA CMPK2 benefits HCV replication by negatively regulating ISGs (11). We recently observed that lncRNA NORAD is upregulated in HCV infected hepatocytes (12), although modulation of NORAD has no detectable effect on HCV growth.

From the published reports (9, 12), we initially selected serval lncRNAs to study their role in the context of HCV replication. Linc-Pint is the only lncRNA in our initial screening shown reduced expression in HCV infected hepatocytes and HCV infected liver specimens. Linc-Pint is located at chromosome 7q32.3 region and trans-activated by p53 (13). The role of Linc-Pint in HCV infected hepatocytes and regulation of host response to liver disease progression remains largely unknown. In this study, we demonstrated that exogenous expression of Linc-Pint inhibits HCV replication and virus induced lipogenesis through interaction with RNA binding protein SRPK2.

Materials and Methods

Tissue samples

Chronic HCV infected liver tissue biopsy specimens and other (non-viral) chronic liver disease tissue samples were acquired from patients through IRB approval at the Saint Louis University (IRB protocol #27805). All tissue samples were preserved at −80°C until RNA extraction was performed. The study was approved by the Ethics Committee of Saint Louis University and the written informed consent was obtained from all patients.

Cell culture, Transfection and Infection

Immortalized human hepatocytes (IHH) and Huh7 cells were maintained in Dulbecco's modified Eagle's medium (DMEM) supplemented with 10% fetal bovine serum (FBS) and 1% penicillin/streptomycin at 37°C in a 5% CO_2 atmosphere. IHH and Huh7 cells were seeded into 6-well plate at a density of 3×10^5 cells/well and transfected with 1μg/well of empty vector or pcDNA3 Linc-Pint plasmid DNA (Accession No.- BC130416) using lipofectamine (Invitrogen). Cells were harvested for RNA and protein analyses.

HCV genotype 2a (clone JFH1) was grown in Huh7.5 cells as described previously (14). Culture supernatant containing released HCV particle was filtered through a 0.45μm pore size cellulose acetate membrane (Nalgene) to remove cell debris and quantitated in standard IU/mL. For infection, IHH and Huh7 cells were incubated with HCV JFH1, and cells were harvested for RNA and protein analyses.

To evaluate the role of Linc-Pint overexpression on HCV replication, Huh7 cells were transfected with control (empty vector pcDNA3) and pcDNA3-Linc-Pint plasmid DNA, and infected with HCV JFH1-GFP (15, 16). Cells were examined ~48 hr post-infection using a fluorescent microscope. Transfection of SRPK2 small interfering RNA (siRNA) into IHH and Huh7 cells was performed using lipofectamine RNAiMAX (Invitrogen). Briefly, IHH and Huh7 cells were transfected with 50 nM SRPK2 siRNA (sc-39237; Santa Cruz Biotechnology) or control siRNA. After 48 hr of transfection, cells were harvested for RNA and protein analyses.

Deletion mutant constructs of Linc-Pint

Linc-Pint gene fragments of the deletion mutant (Linc-Pint-A and Linc-Pint-B) were PCR amplified from pcDNA3 Linc-Pint plasmid (Accession No.- BC130416) using specific primers (Table 1). Fragments were digested with BamHI and XhoI restriction enzymes and cloned into pcDNA3 plasmid. Full length Linc-Pint plasmid and deletion mutant constructs were used for RNA Pull-down assay using sense or anti-sense RNA followed by Western blot analysis to examine the presence of specific protein in eluted samples as described below. Linc-Pint constructs were transfected into IHH and Huh7 cells for protein analysis.

RNA isolation and Quantitative Real-time PCR

Total RNA was isolated using TRIzol reagent (Invitrogen) from different conditions and complementary DNA (cDNA) was generated by reverse transcription with random hexamers and a Superscript III reverse transcriptase kit (Invitrogen). For quantification of gene expression, real-time PCR (qRT-PCR) was performed with a 7500 real-time PCR system using SYBR-Green PCR master-mix and specific primer pairs (Table-1). 18s ribosomal RNA (18s rRNA) was used as an internal control. HCV quantitation was performed as described previously (17). The relative gene expression was analysed by the $2^{-\Delta\Delta CT}$ formula ($\Delta\Delta CT = \Delta CT$ of the sample – ΔCT of the untreated control).

Western Blot analysis

Mock-infected, HCV-infected, or control siRNA- or specific siRNA-treated cells, control empty vector or Linc-Pint overexpressed virus-infected cells were lysed in a sample buffer,

subjected to SDS-PAGE, and transferred onto a nitrocellulose membrane.. The membrane was blocked in 5% non-fat dried milk and incubated with specific primary antibody for overnight at 4°C followed by incubation with secondary antibody conjugated with horseradish peroxidase (HRP) for 1 hr. Proteins were detected by an enhanced chemiluminescence Western blot substrate (ThermoFisher Scientific). In a different set of experiment, IHH or Huh7 cells expressing Linc-Pint treated with vehicle or predetermined dose of MG132 (20 uM) for 6 hr. Cell lysates were analyzed by Western blot analysis for SRPK2 expression using specific antibody. Membranes were reprobed with HRP conjugated β-actin or tubulin antibody (Santa Cruz Biotechnology) to determine the protein load as internal control. Densitometric analysis of protein band images was performed using ImageJ software. Commercially available antibodies to SRPK2, (611118, BD bioscience), phosphoSRPK2 (Ser494, 07–1817, Millipore), pan phosphor-DR protein (MABE50, Millipore), fatty acid synthase (FASN) (A-5, Santa Cruz), ATP-Citrate Lyase (D1X6P, Cell signalling) were used for Western blot analysis.

RNA Pull-down and Mass Spectrometry

Linc-Pint sense or anti-sense RNA was *in vitro* transcribed from pcDNA3 Linc-Pint plasmid (500 ng) using biotin RNA labelling mix and T7 or SP6 RNA polymerase (AmpliScribe T7-Flash Transcription kit, Lucigen) according to manufacturer's instruction. Purified biotinylated sense or anti-sense RNA (20 pmol) was labelled with streptavidin magnetic beads (Pierce, ThermoFisher Scientific) for 1 hr in rotor at room temperature. Huh7.5 cells harbouring the genome-length HCV replicon (Rep2a) were lysed in IP buffer (25mM Tris-HCL pH-7.5, 150mM NaCl, 1mM EDTA, 5% Glycerol, 1% NP40, 1x Protease Inhibitor, and 100U/ml RNase Inhibitor) and RNA-pull down assay was performed by Pierce Magnetic RNA-Protein Pull-Down Kit (Thermo Fisher Scientific). In brief, the cell lysates (5 mg) were incubated with the beads containing sense or anti-sense RNA for 3 hr at 4°C. After washing the beads, the bound proteins were eluted by elution buffer at 37°C for 1hr with agitation. The eluted proteins were used for Mass spectrometric analysis. The mass spectrometer used for data acquisition is a Thermo Q-Exactive system. Peptides were separated on an EASYnLC system with a Thermo ES803 PepMap C18 column; data was acquired in DDA mode (data dependent acquisition; top10 m/z for MS2 per cycle). Candidate proteins were defined as those have at least 2-fold enrichment at sense strand as compared to anti-sense RNA pull-down. In another set of experiment, the beads containing RNA was incubated with extracts of IHH followed by the Western blot analysis to determine the presence of specific protein in eluted samples.

RNA Immunoprecipitation

IHH were transfected with pcDNA3 Linc-Pint plasmid and cells were lysed after 24 hr of transfection with specific IP buffer (25mM Tris-HCL pH-7.5, 150mM NaCl, 1mM EDTA, 5% Glycerol, 1% NP40, 1x Protease Inhibitor, and 100 U/ml RNase Inhibitor). Cell lysate were centrifuged and incubated overnight with 1 μg of antibody against SRPK2 (sc-390534) or the isotype control antibody at 4°C. Cell lysates were incubated with protein G Sepharose beads (Amersham biosciences) for 2 hr. After washing, RNA was isolated from beads using TRIzol reagent and cDNA was synthesized and relative expression of Linc-Pint was examined by qRT-PCR as described above.

Proliferation assay

IHH and Huh7 cells were seeded in a 35mm dish at a density of 10^4 cells/dish and transfected with 1μg/dish of control empty vector (pcDNA3) or pcDNA3 Linc-Pint plasmid DNA. Cells were harvested at different time points and cell number was counted by Trypan blue exclusion method. The proliferation assay was repeated at least three times.

Lipid Droplet staining

Huh7.5 cells were transfected with pcDNA3 vector (control) or pcDNA3 Linc-Pint plasmid and after 24 hrs, cells were stained with 2.5 μg/ml of BODIPY 493/503 (Invitrogen) for 1 hr. After washing, the cells were counter stained with Hoechst dye (5 μg/ ml) for nuclear staining. Lipid droplets were examined by using an inverted fluorescent microscope.

Statistical analysis

All the experiments were performed at least in triplicates and data were presented as mean ± standard deviation. Statistical analysis was performed by the Student's t-test with a two-tailed distribution. P value < 0.05 was considered statistically significant.

Results

Linc-Pint is downregulated in HCV infected hepatocytes

Huh7 cells were infected with HCV JFH1 (moi-1.0), and total RNA was isolated 60 hr post-infection. RNA from mock treated cells were used as a negative control. Linc-Pint expression was significantly reduced in HCV infected hepatocytes as compared to mock treated control cells (Fig. 1, panel A). RNA from Huh7.5 cells or Huh 7.5 cells harbouring genome-length HCV (Rep2a) was also compared for Linc-Pint expression. A significant downregulation of Linc-Pint expression in Rep2a cells was observed (Fig. 1, panel B). To examine the status of Linc-Pint in another flavivirus, we examined Linc-Pint expression from RNA of keratinocytes and macrophages mock treated or infected with Zika virus. We did not observe an alteration of Linc-Pint, although Zika virus infection was established, as measured by qRT-PCR (data not shown). We further examined Linc-Pint expression from the chronic HCV infected human liver biopsy specimens and non-viral liver biopsy specimens and observed reduced expression of Linc-pint (Fig. 1, panel C).

Linc-Pint overexpression inhibits cell proliferation

Next, we examined the effect of Linc-Pint on cell proliferation. Control empty vector (pcDNA3) or Linc-Pint plasmid DNA was transfected into IHH or Huh7 cells, cell numbers were counted using Trypan blue exclusion method. We observed a significant inhibition of cell proliferation in both IHH and Huh7 cells transfected with Linc-Pint as compared to the vector transfected control cells (Fig. 1, panel D).

Linc-Pint binds with SRPK2 protein

Linc-Pint is transcriptionally induced by p53, and by interacting with PRC2, it inhibits cancer cell migration and invasion (18). However, very little is known about interacting proteins of Linc-Pint, especially in context to virus infection. To identify the interacting

partners of Linc-Pint, we performed RNA pull down assay using biotin-labelled sense and antisense RNA of Linc-Pint, and the complex was analysed by mass spectrometry. To graphically represent our proteomics data, volcano plot–log10(P value) vs. log2(fold) change of sense/antisense spectrum counts was constructed to display the quantitative data (Fig. 2, Panel A-left panel). We identified that SRPK2 protein is one of the interacting partners with high spectral count in Linc-Pint sense strand as compared to anti-sense strand (11.8-fold) in mass spectrometric analysis (Fig. 2, Panel A-right). SRPK2 has been identified to phosphorylate the serine/arginine-rich (SR) proteins involved in splicing of pre-mRNAs and thus regulating the pre-mRNA processing, maturation and stability (19). SRPK2 is highly expressed in many cancers, and plays also important role in tumor progression and metastasis (20, 21). We next verified the RNA-protein interaction using the biotinylated sense or antisense Linc-Pint RNA pulled down from IHH lysates, followed by Western blot analysis with SRPK2 antibody. We observed the association of SRPK2 protein with sense strand of Linc-Pint in hepatocytes (Fig. 2, Panel B). To further confirm the interaction between Linc-Pint and SRPK2, we performed reciprocal immunoprecipitation assay using SRPK2 antibody or the isotype control antibody in Linc-Pint overexpressing IHH followed by qRT-PCR using specific primers. A significant enrichment of Linc-Pint RNA was observed from the RNA of SRPK2 antibody immunoprecipitates using IHH or Huh7 cells, as compared to that of isotype control antibody (Fig. 2, Panel C). Together these data suggested that Linc-Pint interacts with SRPK2 protein.

Linc-Pint overexpression downregulates SRPK2 expression in hepatocytes

Next, we examined the status of SRPK2 in Linc-Pint overexpressing hepatocytes. For this, Linc-Pint or control plasmid DNA was transfected into IHH and Huh7 cells. Cell lysates were analysed by western blot using specific antibody. A significant downregulation in SRPK2 protein level was observed in Linc-Pint overexpressing cells (Fig. 2, Panel D). However, we did not observe an alteration of SRPK2 mRNA level in Linc-Pint overexpressing cells (Fig. 2, Panel E). We next examined whether Linc-Pint overexpression alters the stability of SRPK2. For this, Linc-Pint overexpressing IHH or Huh7 cells treated with vehicle (DMSO) or MG132 proteasome inhibitor. Our result showed the relieve of SRPK2 inhibition following MG132 treatment in the presence of Linc-Pint (Fig. 2, Panel F), indicating that Linc-Pint may downregulate SRPK2 expression at the protein level via proteasomal degradation, although further work is necessary to elucidate the mechanism.

We further identified the specific region on the Linc-Pint gene responsible for SRPK2 interaction. The predicted protein binding site is within 651– 702 nt region of Linc-Pint using *in silico* catRAPID algorithm [tartaglialab.com]. We generated two deletion mutant constructs of Linc-Pint gene, Linc-Pint-A (position 635nt to 1157nt, fragment length- 522 nt) and Linc-Pint-B (position 904nt to 1157nt, fragment length-253 nt) and cloned into pcDNA3 plasmid (Fig. 2, Panel G). RNA Pull-down assay followed by Western blot analysis using sense or antisense of deletion mutant constructs indicated that Linc-Pint-A interacts with SRPK2 (Fig. 2, panel G). We further observed that transfection of Linc-Pint-A inhibits SRPK2 expression like full length construct (Fig. 2, panel H), suggesting Linc-Pint-SRPK2 interacting sites resides between 635–904 nt region.

Linc-Pint inhibits lipogenesis pathway

The primary function of SRPK2 protein is to phosphorylate the serine/arginine rich proteins (SR proteins) involved in pre-mRNA splicing mechanism in mammalian cells (22, 23). SRPK2 induces the efficient splicing of different genes of lipogenesis pathway such as fatty acid synthase (FASN), ATP citrate lyase (ACLY) by phosphorylating SR proteins which results in an increase in the expression of these genes at both mRNA and protein levels (19). We therefore hypothesized that Linc-Pint inhibits the expression of lipogenesis genes by inhibiting SRPK2. For this, we examined the mRNA expression of FASN and ACLY in control empty vector or Linc-Pint overexpressed IHH and Huh7 cells by qRT-PCR. Our result indicated that Linc-Pint overexpression significantly downregulates FASN and ACLY mRNA levels in hepatocytes (Fig. 3, Panels A and B). We further observed a significant inhibition of FASN and ACLY protein levels in Linc-Pint overexpressed IHH and Huh7 cells (Fig. 3, Panels C and D). Reduced lipogenesis results in less lipid droplet (LD) accumulation. To examine the effect of Linc-Pint on LD formation, we labelled the control (empty vector) or Linc-Pint transfected cells with BODIPY and observed significant downregulation of LD formation in Linc-Pint overexpressed hepatocytes (Fig. 3, Panel E), as expected. Together these data suggested that Linc-Pint is inhibiting *de novo* lipogenesis in hepatocytes.

Inhibition of SRPK2 downregulates lipogenesis pathway

Next, we examined the role of SRPK2 protein on the expression level of genes involved in the lipogenesis pathway by depleting SRPK2 in hepatocytes. Control siRNA or siRNA to SRPK2 transfected cell lysates displayed a significant inhibition of SRPK2 expression at the protein level as compared to control cell lysates (Fig. 4, Panel A). Downregulation of FASN or ACLY protein expression in siSRPK2 transfected cells compared to control was also noted (Fig. 4, Panel A). We further observed a significant downregulation of FASN and ACLY mRNA expression in SRPK2 knockdown hepatocytes (Fig. 4, panel B). Our result demonstrated that SRPK2 is involved in the regulation of lipogenesis pathway in hepatocytes.

Effect of Linc-Pint on SRPK2 and FASN expression in HCV infected hepatocytes

We and others have shown that HCV infection induces *de novo* lipogenesis pathway in hepatocytes (16, 24, 25). We therefore hypothesized that Linc-Pint restricts HCV replication by downregulating lipogenesis pathway in hepatocytes. To test our hypothesis, control empty vector or Linc-Pint overexpressed IHH and Huh7 cells were infected with HCV JFH1 (moi=1.0). Cell lysates were examined for expression of SRPK2 and FASN. Our result indicated that HCV infection enhances SRPK2 and FASN expression which are significantly downregulated in Linc-Pint overexpressed HCV infected cells as compared to control vector transfected HCV infected cells (Fig. 5, Panel A). We also observed the inhibition of FASN and ACLY in Linc-Pint transfected Huh7.5 cells harbouring full-length HCV genome (Rep2a) (Fig. 5, Panel B). Together these data suggested that Linc-Pint can downregulate HCV infection by inhibiting lipogenic pathway.

We further examined whether overexpression of Linc-Pint modulates SRPK2 kinase activity. Serine-arginine (SR) proteins are a family of functionally and structurally related splicing

factors that are involved in pre-mRNA splicing. The RS domain of SR proteins is predominantly phosphorylated by two families of protein kinases, namely the SRPKs and Cdc2-like kinases (26). SRPK2 utilizes the same docking groove for the interaction and phosphorylation of SR proteins. For this, we examined the SR-phosphoprotein expression using pan-phospho-SR antibody in Linc-Pint overexpressing cells. Our results showed that decreased phosphorylation of most of the SR-proteins in Linc-Pint overexpressing IHH or Huh7 cells (Fig. 5, **Panel C**). We further examined the status of phospho-SRPK 2 using specific antibody in Western blot analysis. As expected, we observed reduced phosphorylation of SRPK2 (Fig. 5, **Panel C**), since we also observed total SRPK2 expression is lower in Linc-Pint overexpressing hepatocytes.

Overexpression of Linc-Pint limits HCV replication

We next examined whether overexpression of Linc-Pint influences HCV replication. For this, Huh7 cells were transfected with control empty vector or Linc-Pint expressing plasmid DNA and infected with HCV JFH1 (moi=1.0). Total RNA was isolated, and HCV replication was measured by qRT-PCR. We observed overexpression of Linc-Pint inhibits HCV replication (Fig. 5, Panel D). We next performed similar experiment using GFP-tagged HCV and observed lower GFP expression in Linc-Pint overexpressing Huh7 cells as compared to vector control transfected cells (Fig. 5, Panel E). We also depleted SRPK2 using specific siRNA and observed inhibition of HCV replication in genome-length harbouring Huh7.5 cells (Fig. 5, Panel F), in agreement with earlier observation (27). Together these results suggested that exogenous expression of Linc-Pint restricts HCV replication.

Discussion

In this study, we observed that Linc-Pint expression is reduced in HCV infected hepatocytes and liver tissues of chronic HCV infected patients. We identified SRPK2 as an interacting partner of Linc-Pint and overexpression of Linc-Pint inhibits lipogenesis by inhibiting SRPK2 expression. We further demonstrated that HCV mediated enhancement of lipogenesis can be restricted by exogenous expression of Linc-Pint (Fig. 6).

LncRNA is an emerging field of investigation due to their active involvement in cellular proliferation, regulation of gene expression and development of different types of disease progression. Expression of Linc-Pint is found to be deregulated in different types of cancer including gastric cancer, non-small cell lung cancer and renal cancer (28–30). However, very little is known about role of Linc-Pint in the context to HCV infection and HCV associated disease. We observed that Linc-Pint expression is reduced in HCV infected hepatocytes and virus infected liver tissue specimens. Although Linc-Pint expression was not altered in Zika virus infected cells, it will be interesting to examine the status of Linc-Pint in hepatitis A or hepatitis B virus infected cells in future study. To identify the interacting partner of Linc-Pint in presence of HCV, we performed RNA- pull down and proteomics in HCV replicating hepatocytes. SRPK2 is identified as one of the Linc-Pint interacting proteins. SRPK2 is a key regulator of RNA-binding SR proteins. SRPK2 is overexpressed in different types of cancers including acute myeloid leukaemia, colon and lung cancer (20, 31, 32). The major

function of SRPK2 is to efficiently phosphorylate at the arginine/serine (RS) domains present in serine/arginine (SR) proteins involved in splicing of pre-mRNAs. It can also regulate splice site selection, spliceosome assembly and cellular redistribution of SR proteins and thus is involved in active splicing and maturation of mRNAs (23, 33, 34). SRPK2 regulates the expression of lipogenic enzymes by inducing efficient splicing of their mRNAs (19). RNA binding function of SRPK2 was reported earlier (35), although the binding domain was not mapped. By *in-silico* analysis [catRAPID fragments algorithm; http://service.tartaglialab.com] we predict that the 276–402 region of SRPK2 contains interaction propensity with Linc-Pint and need verification from further study.

Linc-Pint is positively regulated by p53, and inhibits cancer cell migration and invasion by interacting with PRC2 (18). PRC2 was present in our proteomics dataset, however, spectrum count of PRC2 with antisense strand of Linc-Pint was high, suggesting non-specific association in our system. Further there is no report discussing the role of PRC2 in HCV replication or pathogenesis.

Since we observed significant downregulation of SRPK2 in Linc-Pint overexpressed hepatocytes, we examined the genes involved in lipid metabolism pathway in IHH and Huh7 cells. Linc-Pint overexpression also significantly inhibited FASN and ACLY expression both at the mRNA and protein levels. As expected, knockdown of SRPK2 in IHH or Huh7 cell lines inhibits FASN and ACLY expression. Lipogenesis is altered in many cancers. Highly proliferative cancer cells consume high levels of substrates for their growth which leads to induced lipogenesis in cancer cells (34). FASN is the key enzyme of this pathway which is found to be highly expressed in many cancers (36, 37). Inhibition of this enzyme can be a therapeutic option for treatment of cancer (38, 39).

Several reports suggested that lipid biosynthesis plays an important role in HCV replication (25, 40–42). Furthermore, HCV induced lipogenesis contributes to the increased accumulation of lipid droplets (LDs) in cell which facilitates virus assembly and secretion (16, 43). In this study, we showed that HCV RNA replication was significantly downregulated upon Linc-Pint overexpression. On the other hand, Linc-Pint overexpression significantly reduced the *de novo* lipogenesis and LD accumulation in hepatocytes. Together our results indicated that Linc-Pint may modulate at different stages of HCV life cycle by downregulating *de novo* lipogenesis in hepatocytes.

HCV enhances its replication by modulating lipid metabolism in host cells. Increased lipogenesis may also contribute to HCV induced liver damages by inducing liver steatosis due to enhanced lipid accumulation in liver (44–46). Linc-Pint overexpression significantly reduced the LD accumulation in hepatocytes. HCV mediated enhancement of SRPK2 and FASN can be controlled by overexpression of Linc-Pint. HCV life cycle is also found to be dependent on host RNA processing machinery including phosphorylation by SR protein and their regulators such as SRPKs. In fact, overexpression of SRPK2 leads to significant augmentation of HCV replication whereas knockdown of SRPK2 results in downregulation of HCV replication (27). Therefore, we postulate that Linc-Pint and SRPK2 form complex in regulating hepatic lipogenesis.

It is intriguing to consider that HCV infection downregulates Linc-Pint-SRPK2 axis resulting in dysregulated lipid metabolism. We observed that Linc-Pint is downregulated in HCC from non-alcoholic fatty liver disease (data not shown). Therefore, exogenous delivery of Linc-Pint alleviates a promising avenue for developing interventional strategies in prevention of not only HCV associated HCC, also from other etiology.

In conclusion, we identified lncRNA Linc-Pint is downregulated in HCV infected hepatocytes. We identified SRPK2 is an interacting partner of Linc-Pint which plays an important role in lipogenesis. Our data strongly suggested that HCV mediated downregulation of Linc-Pint enhances SRPK2 which enhances lipogenesis and exogenous expression of Linc-Pint limits HCV mediated enhancement of SRPK2 and lipogenic molecules. How HCV downregulates Linc-Pint is yet to be determined. Linc-Pint is a p53 regulated lncRNA (13). One possibility is that HCV inhibits Linc-Pint expression in hepatocytes by impairing p53 signalling, although other transcription factors may also have roles and will be examined in future studies. Together our study contributes to the understanding of the previously unexplored role of Linc-Pint in HCV associated liver carcinogenesis.

Acknowledgment

We thank Dr. Oskar Marín-Béjar for providing Linc-Pint plasmid DNA. The mass spectrometric experiments were designed and performed at the Washington University Proteomics Shared Resource (WU-PSR), Dr. R. Reid Townsend, Director. The WU-PSR is supported in part by the WU Institute of Clinical and Translational Sciences (NCATS UL1 TR002345), the Mass Spectrometry Research Resource (NIGMS P41 GM103422) and the Siteman Comprehensive Cancer Center Support Grant (NCI P30 CA091842). We thank Rajeev Aurora for helping with volcano graph and Anutosh Chakraborty for helping with SRPK2 kinase activity.

Financial Support: This work was supported by the National Institutes of Health (DK081817 to R.B.R.; DK113645 to R.R and RBR).

List of abbreviations:

18 rRNA	18s ribosomal RNA
ACLY	ATP-Citrate lyase
cDNA	Complementary DNA
DMEM	Dulbecco’s modified Eagle’s medium
FASN	Fatty acid synthase
FBS	Fetal bovine serum
GFP	Green fluorescent protein
HCC	Hepatocellular carcinoma
HCV	Hepatitis C virus
HRP	Horseradish peroxidase
IHH	Immortalized human hepatocytes

LD	Lipid droplet
Linc-Pint	Long intergenic non-protein coding RNA, p53 induced transcript
LncRNA	Long non-coding RNAs
NcRNAs	Non-coding RNAs
PRC2	Polycomb repressive complex 2
qRT-PCR	Quantitative real-time PCR
siRNA	Small interfering RNA
SR protein	Serine/arginine rich protein
SRPK2	Serine/arginine protein specific kinase 2

References

1. Spizzo R, Almeida MI, Colombatti A, Calin GA. Long non-coding RNAs and cancer: a new frontier of translational research? Oncogene 2012;31:4577–4587. [PubMed: 22266873]
2. Rinn JL, Chang HY. Genome regulation by long noncoding RNAs. Annu Rev Biochem 2012;81:145–166. [PubMed: 22663078]
3. Iyer MK, Niknafs YS, Malik R, Singhal U, Sahu A, Hosono Y, Barrette TR, et al. The landscape of long noncoding RNAs in the human transcriptome. Nat Genet 2015;47:199–208. [PubMed: 25599403]
4. Cipolla GA, de Oliveira JC, Salviano-Silva A, Lobo-Alves SC, Lemos DS, Oliveira LC, Jucoski TS, et al. Long Non-Coding RNAs in Multifactorial Diseases: Another Layer of Complexity. Noncoding RNA 2018;4.
5. Lin C, Yang L. Long Noncoding RNA in Cancer: Wiring Signaling Circuitry. Trends Cell Biol 2018;28:287–301. [PubMed: 29274663]
6. Balas MM, Johnson AM. Exploring the mechanisms behind long noncoding RNAs and cancer. Noncoding RNA Res 2018;3:108–117. [PubMed: 30175284]
7. Plissonnier ML, Herzog K, Levrero M, Zeisel MB. Non-Coding RNAs and Hepatitis C Virus-Induced Hepatocellular Carcinoma. Viruses 2018;10.
8. Barriocanal M, Fortes P. Long Non-coding RNAs in Hepatitis C Virus-Infected Cells. Front Microbiol 2017;8:1833. [PubMed: 29033906]
9. Carnero E, Barriocanal M, Prior C, Pablo Unfried J, Segura V, Guruceaga E, Enguita M, et al. Long noncoding RNA EGOT negatively affects the antiviral response and favors HCV replication. EMBO Rep 2016;17:1013–1028. [PubMed: 27283940]
10. Qian X, Xu C, Zhao P, Qi Z. Long non-coding RNA GAS5 inhibited hepatitis C virus replication by binding viral NS3 protein. Virology 2016;492:155–165. [PubMed: 26945984]
11. Kambara H, Niazi F, Kostadinova L, Moonka DK, Siegel CT, Post AB, Carnero E, et al. Negative regulation of the interferon response by an interferon-induced long non-coding RNA. Nucleic Acids Res 2014;42:10668–10680. [PubMed: 25122750]
12. Sur S, Sasaki R, Devhare P, Steele R, Ray R, Ray RB. Association between MicroRNA-373 and Long Noncoding RNA NORAD in Hepatitis C Virus-Infected Hepatocytes Impairs Wee1 Expression for Growth Promotion. J Virol 2018;92.
13. Marin-Bejar O, Marchese FP, Athie A, Sanchez Y, Gonzalez J, Segura V, Huang L, et al. Pint lincRNA connects the p53 pathway with epigenetic silencing by the Polycomb repressive complex 2. Genome Biol 2013;14:R104. [PubMed: 24070194]

14. Kanda T, Basu A, Steele R, Wakita T, Ryerse JS, Ray R, Ray RB. Generation of infectious hepatitis C virus in immortalized human hepatocytes. J Virol 2006;80:4633–4639. [PubMed: 16611923]
15. Shrivastava S, Devhare P, Sujijantarat N, Steele R, Kwon YC, Ray R, Ray RB. Knockdown of Autophagy Inhibits Infectious Hepatitis C Virus Release by the Exosomal Pathway. J Virol 2016;90:1387–1396. [PubMed: 26581990]
16. Sasaki R, Sur S, Cheng Q, Steele R, Ray RB. Repression of MicroRNA-30e by Hepatitis C Virus Enhances Fatty Acid Synthesis. Hepatol Commun 2019;3:943–953. [PubMed: 31334444]
17. Mukherjee A, Di Bisceglie AM, Ray RB. Hepatitis C virus-mediated enhancement of microRNA miR-373 impairs the JAK/STAT signaling pathway. J Virol 2015;89:3356–3365. [PubMed: 25589644]
18. Marin-Bejar O, Mas AM, Gonzalez J, Martinez D, Athie A, Morales X, Galduroz M, et al. The human lncRNA LINC-PINT inhibits tumor cell invasion through a highly conserved sequence element. Genome Biol 2017;18:202. [PubMed: 29078818]
19. Lee G, Zheng Y, Cho S, Jang C, England C, Dempsey JM, Yu Y, et al. Post-transcriptional Regulation of De Novo Lipogenesis by mTORC1-S6K1-SRPK2 Signaling. Cell 2017;171:1545–1558 e1518. [PubMed: 29153836]
20. Wang J, Wu HF, Shen W, Xu DY, Ruan TY, Tao GQ, Lu PH. SRPK2 promotes the growth and migration of the colon cancer cells. Gene 2016;586:41–47. [PubMed: 27041240]
21. Zhuo YJ, Liu ZZ, Wan S, Cai ZD, Xie JJ, Cai ZD, Song SD, et al. Enhanced expression of SRPK2 contributes to aggressive progression and metastasis in prostate cancer. Biomed Pharmacother 2018;102:531–538. [PubMed: 29587239]
22. Zhou Z, Fu XD. Regulation of splicing by SR proteins and SR protein-specific kinases. Chromosoma 2013;122:191–207. [PubMed: 23525660]
23. Wang HY, Lin W, Dyck JA, Yeakley JM, Songyang Z, Cantley LC, Fu XD. SRPK2: a differentially expressed SR protein-specific kinase involved in mediating the interaction and localization of pre-mRNA splicing factors in mammalian cells. J Cell Biol 1998;140:737–750. [PubMed: 9472028]
24. Bose SK, Kim H, Meyer K, Wolins N, Davidson NO, Ray R. Forkhead box transcription factor regulation and lipid accumulation by hepatitis C virus. J Virol 2014;88:4195–4203. [PubMed: 24478438]
25. Narayanan S, Nieh AH, Kenwood BM, Davis CA, Tosello-Trampont AC, Elich TD, Breazeale SD, et al. Distinct Roles for Intracellular and Extracellular Lipids in Hepatitis C Virus Infection. PLoS One 2016;11:e0156996. [PubMed: 27280294]
26. Long Y, Sou WH, Yung KWY, Liu H, Wan SWC, Li Q, Zeng C, et al. Distinct mechanisms govern the phosphorylation of different SR protein splicing factors. J Biol Chem 2019;294:1312–1327. [PubMed: 30478176]
27. Karakama Y, Sakamoto N, Itsui Y, Nakagawa M, Tasaka-Fujita M, Nishimura-Sakurai Y, Kakinuma S, et al. Inhibition of hepatitis C virus replication by a specific inhibitor of serine-arginine-rich protein kinase. Antimicrob Agents Chemother 2010;54:3179–3186. [PubMed: 20498328]
28. Feng H, Zhang J, Shi Y, Wang L, Zhang C, Wu L. Long noncoding RNA LINC-PINT is inhibited in gastric cancer and predicts poor survival. J Cell Biochem 2019;120:9594–9600. [PubMed: 30569513]
29. Zhang L, Hu J, Li J, Yang Q, Hao M, Bu L. Long noncoding RNA LINC-PINT inhibits non-small cell lung cancer progression through sponging miR-218–5p/PDCD4. Artif Cells Nanomed Biotechnol 2019;47:1595–1602. [PubMed: 31010333]
30. Duan J, Ma X, Shi J, Xuan Y, Wang H, Li P, Zhang Y, et al. Long noncoding RNA LINC-PINT promotes proliferation through EZH2 and predicts poor prognosis in clear cell renal cell carcinoma. Onco Targets Ther 2019;12:4729–4740. [PubMed: 31417274]
31. Gout S, Brambilla E, Boudria A, Drissi R, Lantuejoul S, Gazzeri S, Eymin B. Abnormal expression of the pre-mRNA splicing regulators SRSF1, SRSF2, SRPK1 and SRPK2 in non small cell lung carcinoma. PLoS One 2012;7:e46539. [PubMed: 23071587]

32. Jang SW, Yang SJ, Ehlen A, Dong S, Khoury H, Chen J, Persson JL, et al. Serine/arginine protein-specific kinase 2 promotes leukemia cell proliferation by phosphorylating acinus and regulating cyclin A1. Cancer Res 2008;68:4559–4570. [PubMed: 18559500]
33. Koizumi J, Okamoto Y, Onogi H, Mayeda A, Krainer AR, Hagiwara M. The subcellular localization of SF2/ASF is regulated by direct interaction with SR protein kinases (SRPKs). J Biol Chem 1999;274:11125–11131. [PubMed: 10196197]
34. Long J, Zhang CJ, Zhu N, Du K, Yin YF, Tan X, Liao DF, et al. Lipid metabolism and carcinogenesis, cancer development. Am J Cancer Res 2018;8:778–791. [PubMed: 29888102]
35. Castello A, Fischer B, Eichelbaum K, Horos R, Beckmann BM, Strein C, Davey NE, et al. Insights into RNA biology from an atlas of mammalian mRNA-binding proteins. Cell 2012;149:1393–1406. [PubMed: 22658674]
36. Duan J, Chen L, Zhou M, Zhang J, Sun L, Huang N, Bin J, et al. MACC1 decreases the chemosensitivity of gastric cancer cells to oxaliplatin by regulating FASN expression. Oncol Rep 2017;37:2583–2592. [PubMed: 28339092]
37. Menendez JA, Lupu R. Fatty acid synthase regulates estrogen receptor-alpha signaling in breast cancer cells. Oncogenesis 2017;6:e299. [PubMed: 28240737]
38. Angeles TS, Hudkins RL. Recent advances in targeting the fatty acid biosynthetic pathway using fatty acid synthase inhibitors. Expert Opin Drug Discov 2016;11:1187–1199. [PubMed: 27701891]
39. Menendez JA, Lupu R. Fatty acid synthase (FASN) as a therapeutic target in breast cancer. Expert Opin Ther Targets 2017;21:1001–1016. [PubMed: 28922023]
40. Su AI, Pezacki JP, Wodicka L, Brideau AD, Supekova L, Thimme R, Wieland S, et al. Genomic analysis of the host response to hepatitis C virus infection. Proc Natl Acad Sci U S A 2002;99:15669–15674. [PubMed: 12441396]
41. Kapadia SB, Chisari FV. Hepatitis C virus RNA replication is regulated by host geranylgeranylation and fatty acids. Proc Natl Acad Sci U S A 2005;102:2561–2566. [PubMed: 15699349]
42. Koutsoudakis G, Romero-Brey I, Berger C, Perez-Vilaro G, Monteiro Perin P, Vondran FW, Kalesse M, et al. Soraphen A: A broad-spectrum antiviral natural product with potent anti-hepatitis C virus activity. J Hepatol 2015;63:813–821. [PubMed: 26070407]
43. Miyanari Y, Atsuzawa K, Usuda N, Watashi K, Hishiki T, Zayas M, Bartenschlager R, et al. The lipid droplet is an important organelle for hepatitis C virus production. Nat Cell Biol 2007;9:1089–1097. [PubMed: 17721513]
44. Lerat H, Kammoun HL, Hainault I, Merour E, Higgs MR, Callens C, Lemon SM, et al. Hepatitis C virus proteins induce lipogenesis and defective triglyceride secretion in transgenic mice. J Biol Chem 2009;284:33466–33474. [PubMed: 19808675]
45. Lambert JE, Bain VG, Ryan EA, Thomson AB, Clandinin MT. Elevated lipogenesis and diminished cholesterol synthesis in patients with hepatitis C viral infection compared to healthy humans. Hepatology 2013;57:1697–1704. [PubMed: 23417775]
46. Meng Z, Liu Q, Sun F, Qiao L. Hepatitis C virus nonstructural protein 5A perturbs lipid metabolism by modulating AMPK/SREBP-1c signaling. Lipids Health Dis 2019;18:191. [PubMed: 31684957]

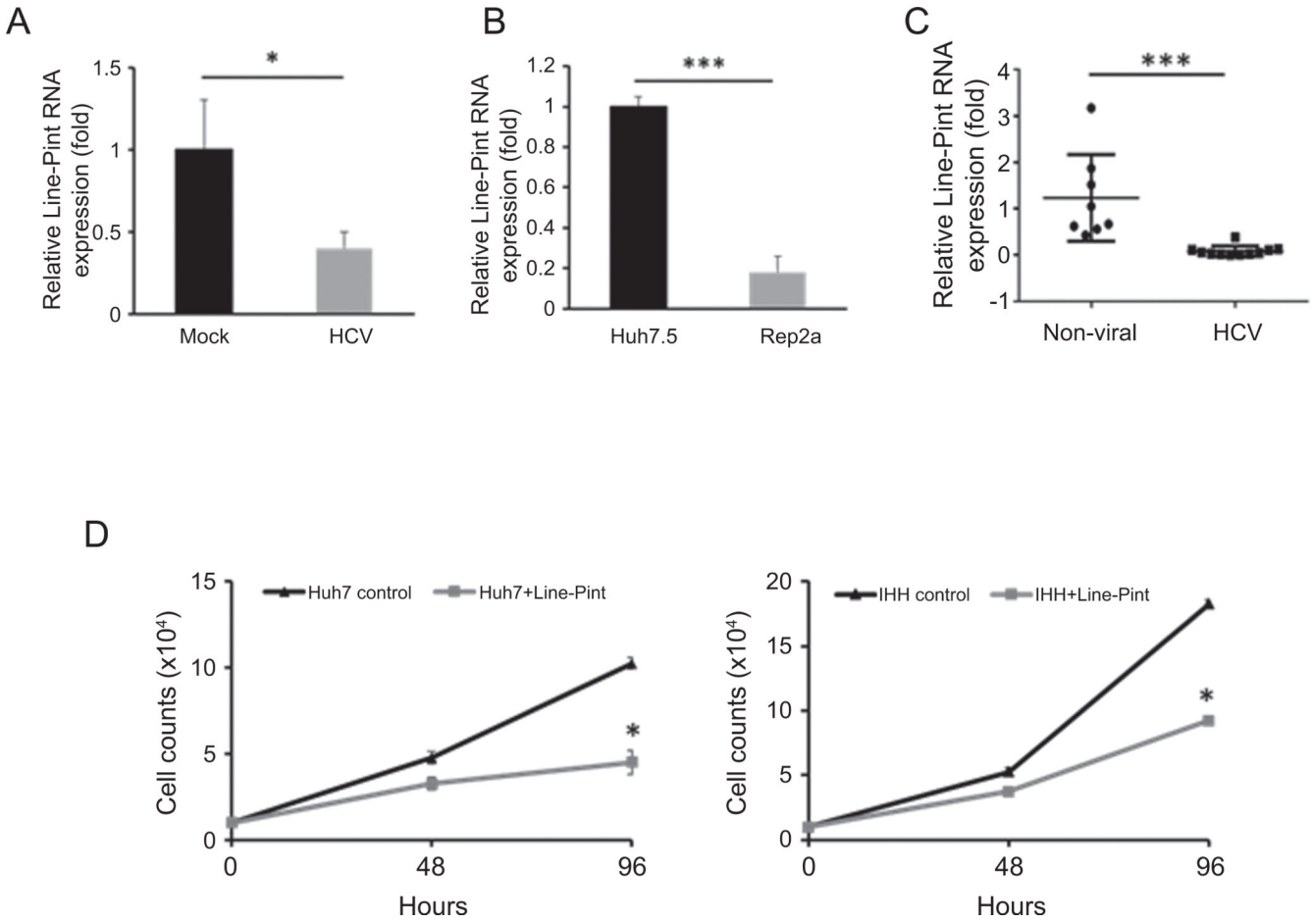

Figure 1: HCV infection downregulates Linc-Pint expression.

(A) Huh7 cells were infected with HCV-JFH1 (moi=1.0). Total RNA was isolated from mock treated or infected cells, and Linc-Pint and 18s rRNA were measured by real-time PCR. (B) RNA from Huh7.5 cells and Huh7.5 cells harbouring genome-length HCV replicon (Rep2a) were also isolated, and Linc-Pint expression was examined by real-time PCR. (C) Linc-Pint expression was examined in RNA from HCV infected liver biopsy specimens (n=11) and compared with non-viral liver biopsy specimens (n=8) by qRT-PCT. (D) Hepatocytes (Huh7 or IHH) were transfected with control (pcDNA3 vector) or pcDNA3-Linc-Pint plasmid DNA. Cell numbers were counted at indicated time points. Values represent data from three independent experiments, mean ± SD. Statistical significance was analysed using a two-tailed Student's t test; *P < 0.05, ***P < 0.001.

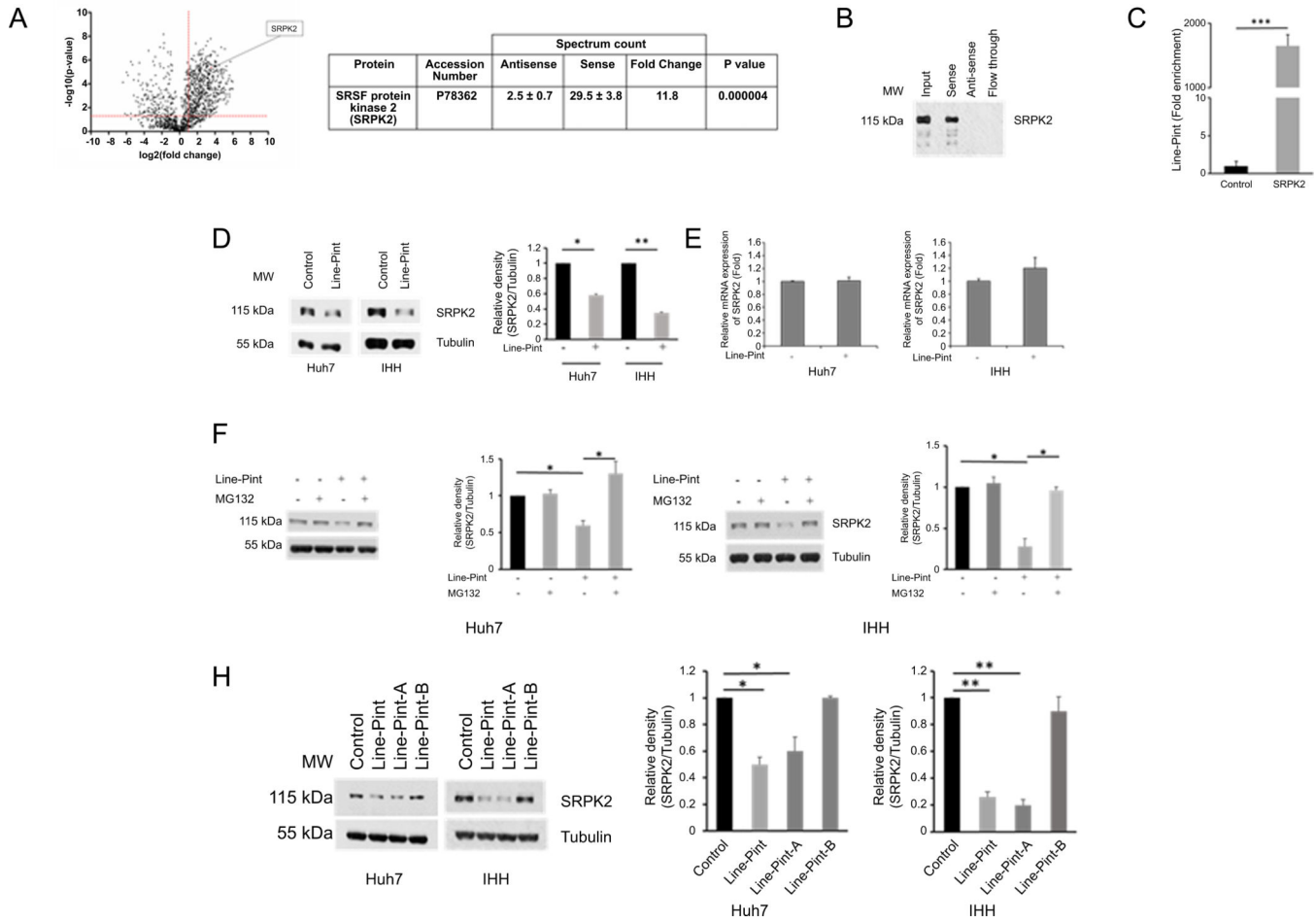

Protein	Accession Number	Spectrum count		Fold Change	P value
		Antisense	Sense		
SRSF protein kinase 2 (SRPK2)	P78362	2.5 ± 0.7	29.5 ± 3.8	11.8	0.000004

Figure 2: Linc-Pint interacts with SRPK2 protein.

(A) The left panel shows a volcano plot from the mass spectrometry data demonstrating magnitude and significance of the proteins interacted with sense strand of Linc-Pint compared with the antisense strand of Linc-Pint. The x-axis is the log2 -fold change value and y axis is −log10 p-value showing statistical significance. Horizontal dashed line showing p =0.05 (−log10(0.05) = 1.3) and vertical dashed line shows the fold change at 2 (log2(2) = 1). The absolute 2-fold change and p-value 0.05 is used as the threshold cut-off. The right panel shows spectrum counts of anti-sense or sense Linc-Pint RNA for SRPK2 from MS. (B) Western blot analysis was performed from sense or anti-sense Linc-Pint RNA pulled-down IHH lysates using specific antibody, and presence of SRPK2 is shown. (C) Cell lysates from Linc-Pint plasmid DNA transfected cells were immunoprecipitated using isotype control or SRPK2 antibody. RNA was isolated from the immunoprecipitates for Linc-Pint expression by qRT-PCR. (D) IHH or Huh7 cells were transfected with control (empty vector) or pcDNA3-Linc-Pint plasmid DNA. Cell lysates were analysed for SRPK2 expression by Western blot using specific antibody. The blot was reprobed with antibody to tubulin for comparison of protein load. Densitometric scanning results are presented as fold in bar diagram. (E) RNA from similar conditions was analysed for SRPK2 expression and normalized by 18s RNA. (F) Linc-pint overexpressing Huh 7 or IHH cells were treated with vehicle (−) or MG132 (20 uM) for 6 h. Cell lysates were analyzed by Western blot using

specific antibody. The blot was reprobed with antibody to tubulin for comparison of protein load. Densitometric scanning results are presented as fold in bar diagram. Statistical significance was analyzed using a two-tailed Student's t test; *P < 0.05. (G) Schematic diagram of full length Linc-Pint gene (1173 nt) and deletion mutant constructs Linc-Pint-A (522 nt) and Linc-Pint-B (253 nt) cloned into pcDNA3 plasmid. Linc-Pint-A, Linc-Pint-B anti-sense or sense RNA pulled-down IHH lysates using specific antibody showed that Linc-Pint-A interacts with SRPK2 (right panel). (H) IHH or Huh7 cells were transfected with control (empty vector), Linc-Pint, Linc-Pint-A, or Linc-Pint-B plasmid DNA. Cell lysates were analysed for SRPK2 expression by Western blot using specific antibody. The blot was reprobed with antibody to tubulin for comparison of protein load. Densitometric scanning results are presented as fold in bar diagram. Statistical significance was analysed using a two-tailed Student's t test; *P < 0.05, **P < 0.01, ***P < 0.001.

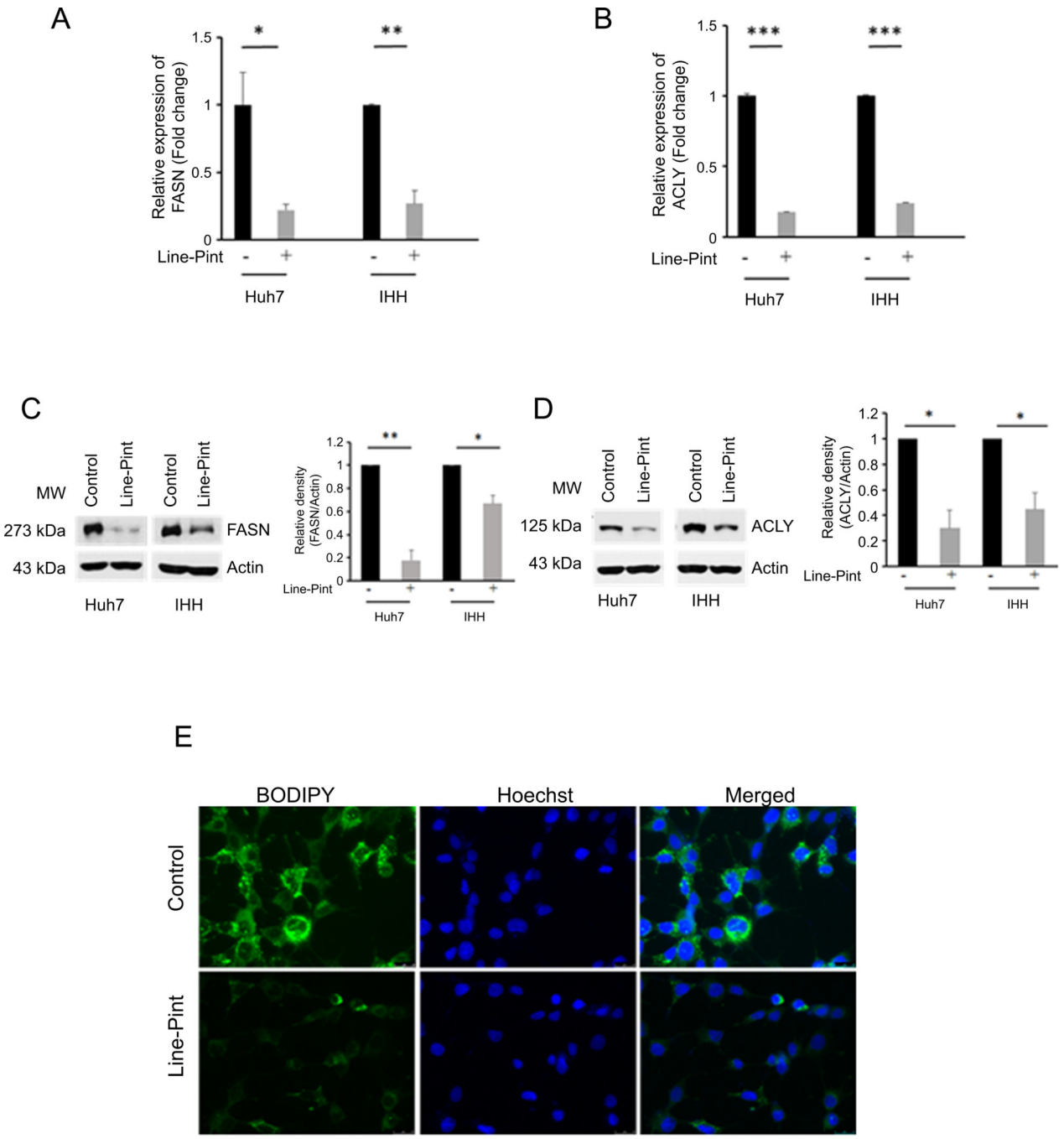

Figure 3: Linc-Pint overexpression in hepatocytes inhibits expression of FASN and ACLY.

IHH and Huh7 cells were transfected with control empty vector (−) or pcDNA3-Linc-Pint plasmid DNA (+). Total RNA was examined for (A) FASN and (B) ACLY expression by qRT-PCR using specific primers. 18s rRNA was used as an internal control. (C and D) IHH and Huh7 cells were transfected with control (empty vector) or Linc-Pint plasmid DNA. Cell lysates were analysed for FASN or ACLY expression by Western blot using specific antibody. The blot was reprobed with antibody to actin for comparison of protein load. Densitometric scanning results are presented as fold in diagrams. Values represent data from

three independent experiments, mean ± SD. (E) Huh7.5 cells were transfected with control (empty vector) or pcDNA3-Linc-Pint plasmid DNA, and cells were stained with BODIPY 493/503 after 24 hr of transfection. LDs were visualized in green colour (BODIPY) and nucleus in blue (Hoechst) by fluorescent microscopy examination in individual and merged image panels. A representative image is shown (40×). Quantitation (measured by ImageJ) of the BODIPY staining is shown in the bar diagram (right panel). Five random fields were counted for LD (green color) +ve cells in 100 cells (blue color). Statistical significance was analysed using a two-tailed Student's t test; *P < 0.05, **P < 0.01, ***P < 0.001.

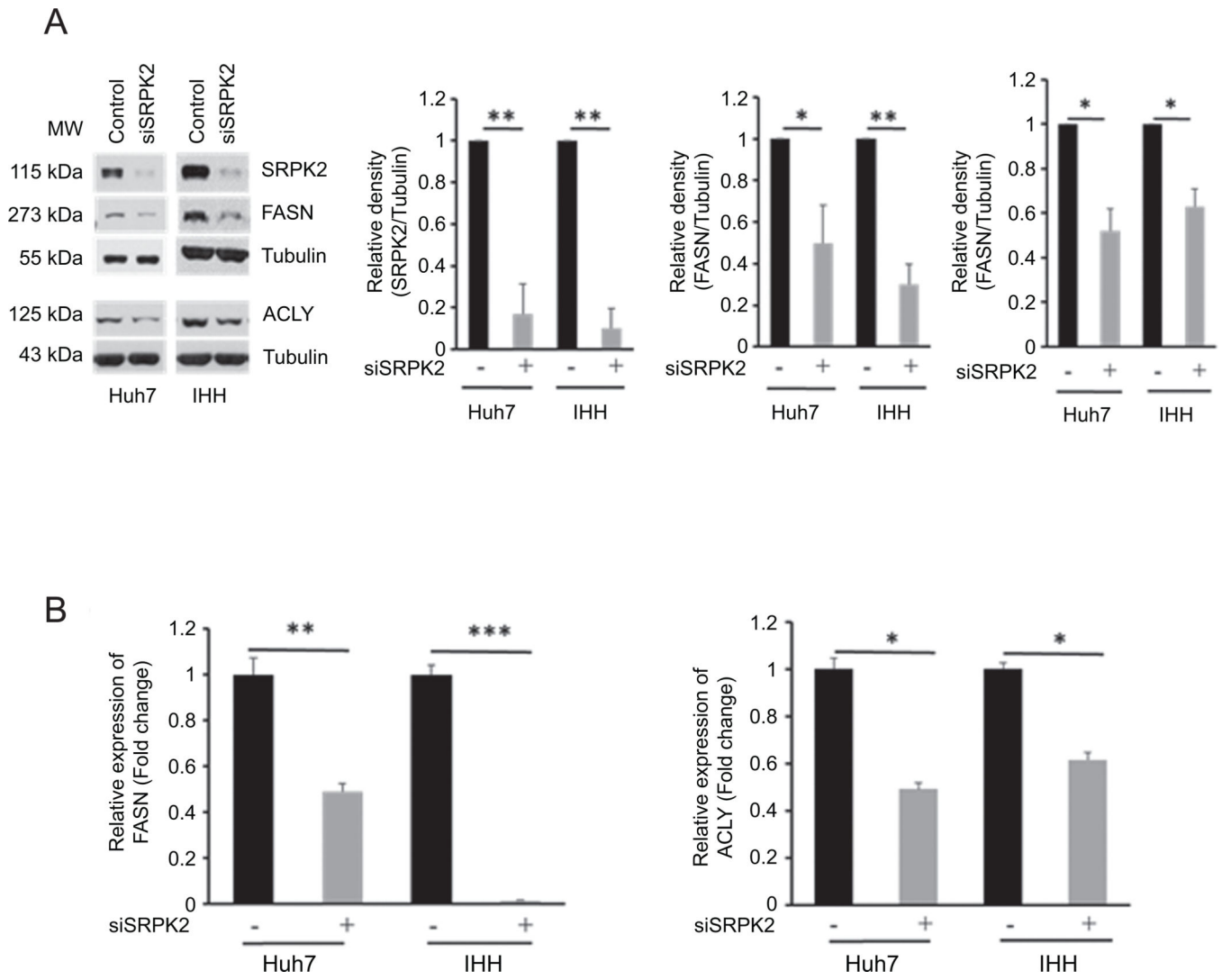

Figure 4: Depletion of SRPK2 downregulates FASN and ACLY expression in hepatocytes.

IHH and Huh7 cells were transfected with control or siRNA to SRPK2. (A) Cell lysates were analysed for SRPK2, FASN and ACLY expression by Western blot using specific antibodies. The blot was reprobed with antibody to tubulin for protein load. Densitometric scanning results are presented as fold in bar diagram. (B) Total RNA was examined for FASN or ACLY expression by qRT-PCR using specific primers. 18s rRNA was used as an internal control. Values represent data from three independent experiments, mean ± SD. Statistical significance was analysed using the two-tailed Student's t test; *P < 0.05, **P < 0.01, ***p<0.001.

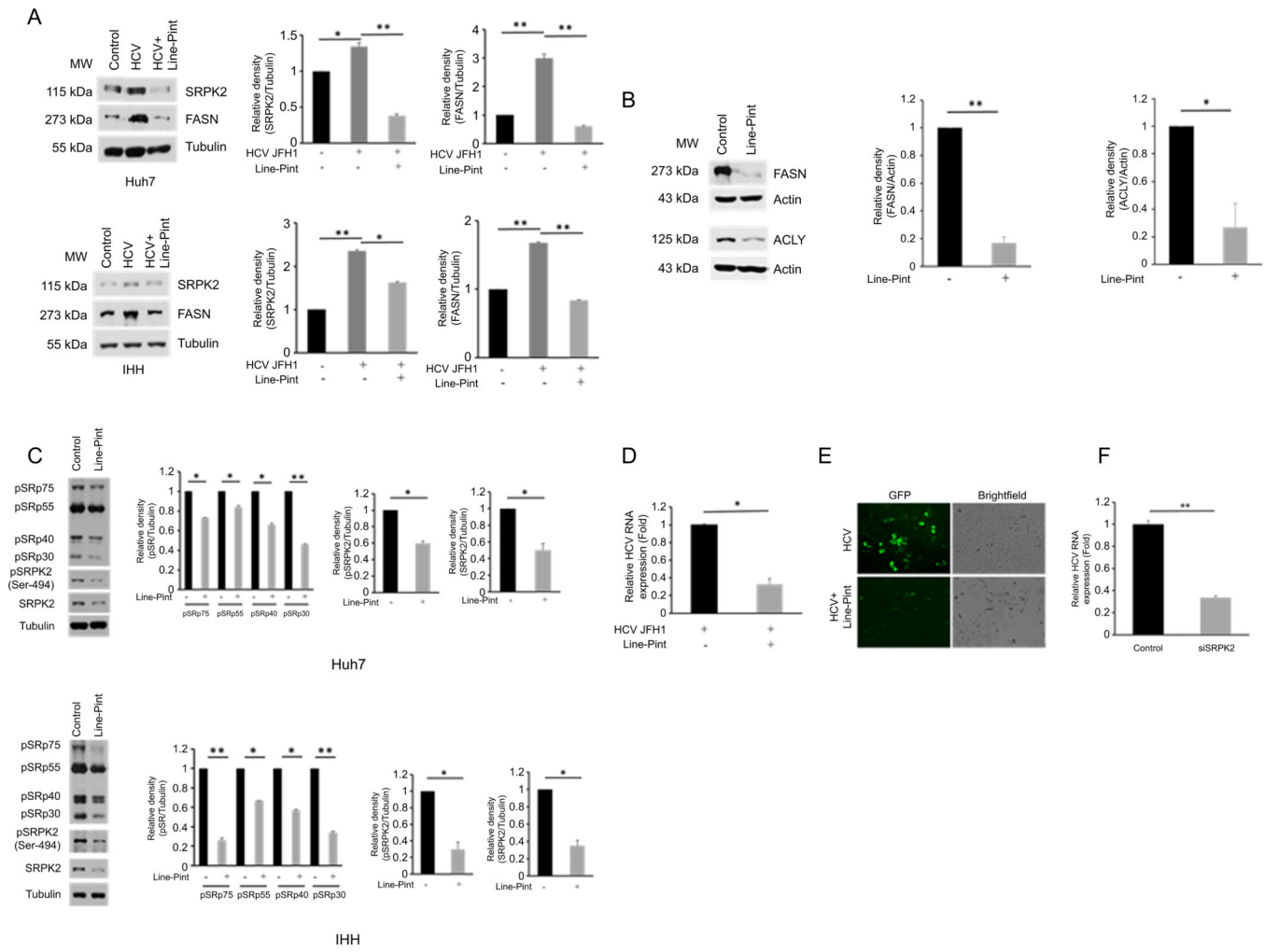

Figure 5: Linc-Pint overexpression limits HCV induced lipogenic molecules and virus replication.

(A) IHH or Huh7 cells were transfected with empty vector control (middle lane) or Linc-Pint plasmid DNA (last lane), and then infected with HCV-JFH1. Mock infected cell lysates were used as control. Cell lysates were analysed for SRPK2 and FASN expression by Western blot using specific antibodies. The blot was reprobed with antibody to tubulin for protein load. Densitometric scanning results are presented as fold in bar diagram. (B) Rep2a cells (HCV replicon) were transfected with control (empty vector) or Linc-Pint plasmid DNA. Cell lysates were analysed for FASN or ACLY expression by Western blot using specific antibody. The blot was reprobed with antibody to actin for comparison of protein load. Densitometric scanning results are presented as fold in bar diagram. (C) Western blot analysis for phospho-SR-proteins using specific antibodies in Huh7 or IHH cell lysates transfected with control (empty vector) or pcDNA3-Linc-Pint plasmid DNA. Blot was reprobed with antibodies to phopso-SRPK2 and total SRPK2. The blot was reprobed with antibody to Tubulin for comparison of protein load. Densitometric scanning results are presented as fold in bar diagrams. (D) Huh7 cells were transfected with empty vector control (−) or Linc-Pint plasmid DNA (+), and infected HCV-JFH1. Virus replication was measured by qRT-PCR. Values represent data from three independent experiments, mean ± SD. (E)

Control (empty vector) or Linc-Pint overexpressed Huh7 cells were infected with GFP-tagged HCV genotype 2a (JFH1-GFP), and virus replication was visualized at 48 hr post infection by fluorescent microscopy. Green color represents the HCV infection (left panel) and bright field is shown (right panel). (F) Rep2a cells (genome length HCV harbouring Huh7.5 cells) were transfected with control siRNA (control) or siRNA to SRPK2 (siSRPK2). Total RNA was examined for HCV RNA expression by qRT-PCR using specific primers. 18s rRNA was used as an internal control. Values represent data from three independent experiments. Statistical significance was analyzed using a two-tailed Student's t test; *$P < 0.05$, **$P < 0.01$.

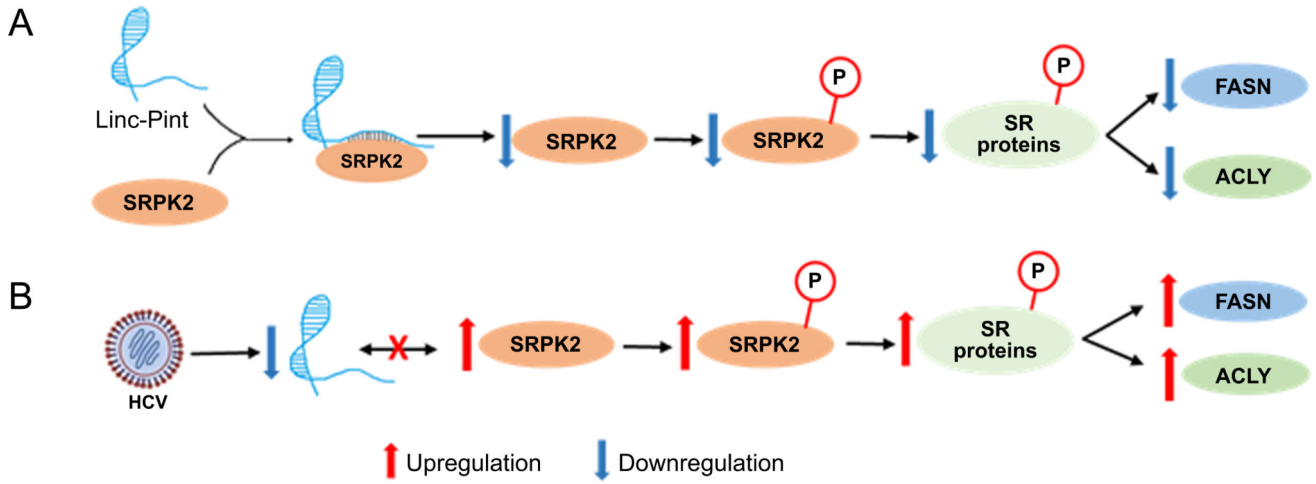

Figure 6: A proposed model of HCV-Linc-Pint-SRPK2 association and lipogenesis.

(A) Linc-Pint physically interacts with SRPK2 and downregulates its expression in the protein level as well as phosphorylation of SR proteins, which leads to decrease expression of FASN and ACLY. (B) HCV infection results in downregulation of Linc-Pint expression, resulting in upregulation SRPK2 expression. Upregulation of SRPK2 expression results in increased *de-novo* lipogenesis by enhancing FASN and ACLY.

Table 1.

List of primes

Primers (PCR)	Sequences
Hs-Linc-Pint	Forward- 5'-CGTGGGAGCCCCTTTAAGTT-3'
	Reverse- 5'-GGGAGGTGGCGTAGTTTCTC-3'
Hs-FASN	Forward - 5′- GCAAGCTGAAGGACCTGTCT-3′
	Reverse - 5′- TCCTCGGAGTGAATCTGGGT-3′
HS-ACLY	Forward - 5′-GACTTCGGCAGAGGTAGAGC-3'
	Reverse - 5′-TCAGGAGTGACCCGAGCATA-3'
Hs-18s	Forward - 5′-GTCATAAGCTTGCGTTGATT-3'
	Reverse - 5′-TAGTCAAGTTCGACCGTCTT-3'
Primers (cloning)	
Linc-Pint-A Forward	5'- CCTCCCCTGGATCCGAGTGCAC -3'
Linc-Pint-B Forward	5'- ACGAGGCAAGGATCCAAAGCAGC-3'
Linc-Pint Reverse	5'- TCTTCCTGGCTCGAGCCTTCCAC -3'